Bioorganic Chemistry 92 (2019) 103244

Contents lists available at ScienceDirect

Bioorganic Chemistry

journal homepage: www.elsevier.com/locate/bioorg

Exploring antidiabetic potential of adamantyl-thiosemicarbazones *via* aldose reductase (ALR2) inhibition

Muhammad Tariq Shehzad[a], Abdul Hameed[b], Mariya al-Rashida[b], Aqeel Imran[c], Maliha Uroos[d], Asnuzilawati Asari[e], Habsah Mohamad[f], Muhammad Islam[a], Shafia Iftikhar[g], Zahid Shafiq[a], Jamshed Iqbal[c]

[a] Institute of Chemical Sciences, Bahauddin Zakariya University, Multan 60800, Pakistan
[b] Department of Chemistry, Forman Christian College (A Chartered University), Ferozepur Road, Lahore 54600, Pakistan
[c] Centre for Advanced Drug Research, COMSATS University Islamabad, Abbottabad Campus, Abbottabad 22060, Pakistan
[d] Institute of Chemistry, University of The Punjab, Lahore 54590, Pakistan
[e] Faculty of Science and Marine Environment, Universiti Malaysia Terengganu, 21030 Kuala Nerus, Terengganu, Malaysia
[f] Institute of Marine Biotechnology, Universiti Malaysia Terengganu, 21030 Kuala Nerus, Terengganu, Malaysia
[g] Department of Chemistry, The University of Lahore, Lahore Pakistan

ARTICLE INFO

Keywords:
Aldose reductase (ALR2)
Adamantyl methyl ketone
Adamantyl-thiosemicarbazone

ABSTRACT

The role of aldose reductase (ALR2) in diabetes mellitus is well-established. Our interest in finding ALR2 inhibitors led us to explore the inhibitory potential of new thiosemicarbazones. In this study, we have synthesized adamantyl-thiosemicarbazones and screened them as aldehyde reductase (ALR1) and aldose reductase (ALR2) inhibitors. The compounds bearing phenyl **3a**, 2-methylphenyl **3g** and 2,6-dimethylphenyl **3m** have been identified as most potent ALR2 inhibitors with IC_{50} values of 3.99 ± 0.38, 3.55 ± 0.26 and 1.37 ± 0.92 μM, respectively, compared with sorbinil (IC_{50} = 3.14 ± 0.02 μM). The compounds **3a**, **3g**, and **3m** also inhibit ALR1 with IC_{50} value of 7.75 ± 0.28, 7.26 ± 0.39 and 7.04 ± 2.23 μM, respectively. Molecular docking was also performed for putative binding of potent inhibitors with target enzyme ALR2. The most potent 2,6-dimethylphenyl bearing thiosemicarbazone **3m** (IC_{50} = 1.37 ± 0.92 μM for ALR2) and other two compound **3a** and **3g** could potentially lead for the development of new therapeutic agents.

1. Introduction

Diabetes mellitus (DM) is among the most chronic ailments; according to an estimate it affects more than half-a-billion people worldwide [1]. The increasing prevalence of DM at an alarming rate is a matter of grave concern [2]. The hyperglycaemic condition, in both type I and II diabetes, is associated with long term complications and dysfunction of vital organs like kidney, heart, nerves and eyes [3,4]. There is an increasing evidence that the pathogenesis of diabetic complications is related to enhanced polyol pathway flux, which in turn is associated with hyperglycaemia due to compromised glucose level in the cells [5,6]. Under normal physiological conditions, the glucose is metabolised to glucose-6-phosphate by hexokinase in the liver during glycolytic pathway, while the polyol pathway flux is activated when glucose concentration increases especially in non-insulin dependent cells [7–9] (see Fig. 1).

Aldose reductase (ALR2) and aldehyde reductase (ALR1) belong to aldo-keto reductase (AKR) superfamily, which is the NADPH dependent family of enzymes mainly responsible for catalysing the reduction of broad range of aldehydes and ketones in the polyol pathway [10]. ALR2, being the first monomeric oxidoreductase enzyme in polyol pathway converts excess glucose into sorbitol in the presence of NADPH as coenzyme and under these conditions, the binding capacity of aldose reductase (ALR2) to glucose enhances significantly [11,12]. Owing to the poor penetration of sorbitol through cell membrane, its accumulation leads to osmotic and oxidative stress, resulting in secondary diabetic complications such as nephropathy, cataract formation, neuropathy, retinopathy and formation of advanced glycation end products (AGEs) [1,4].

In order to control the polyol pathway flux, and hence diabetic complications, the induction of new selective ALR2 inhibitors is highly desirable. Although there are a number of ALR2 inhibitors that have progressed to clinical trials, such as hydantoin derivatives, carboxylic acid derivatives, cyclic imides and others, however to date epalrestat, developed by ONO pharmaceutical, Japan is the only marketed drug (Fig. 2) [13–17]. The non-selective nature of most of the ALR2

E-mail addresses: zahidshafiq@bzu.edu.pk (Z. Shafiq), drjamshed@ciit.net.pk (J. Iqbal).

https://doi.org/10.1016/j.bioorg.2019.103244
Received 17 June 2019; Received in revised form 5 August 2019; Accepted 1 September 2019
Available online 04 September 2019
0045-2068/

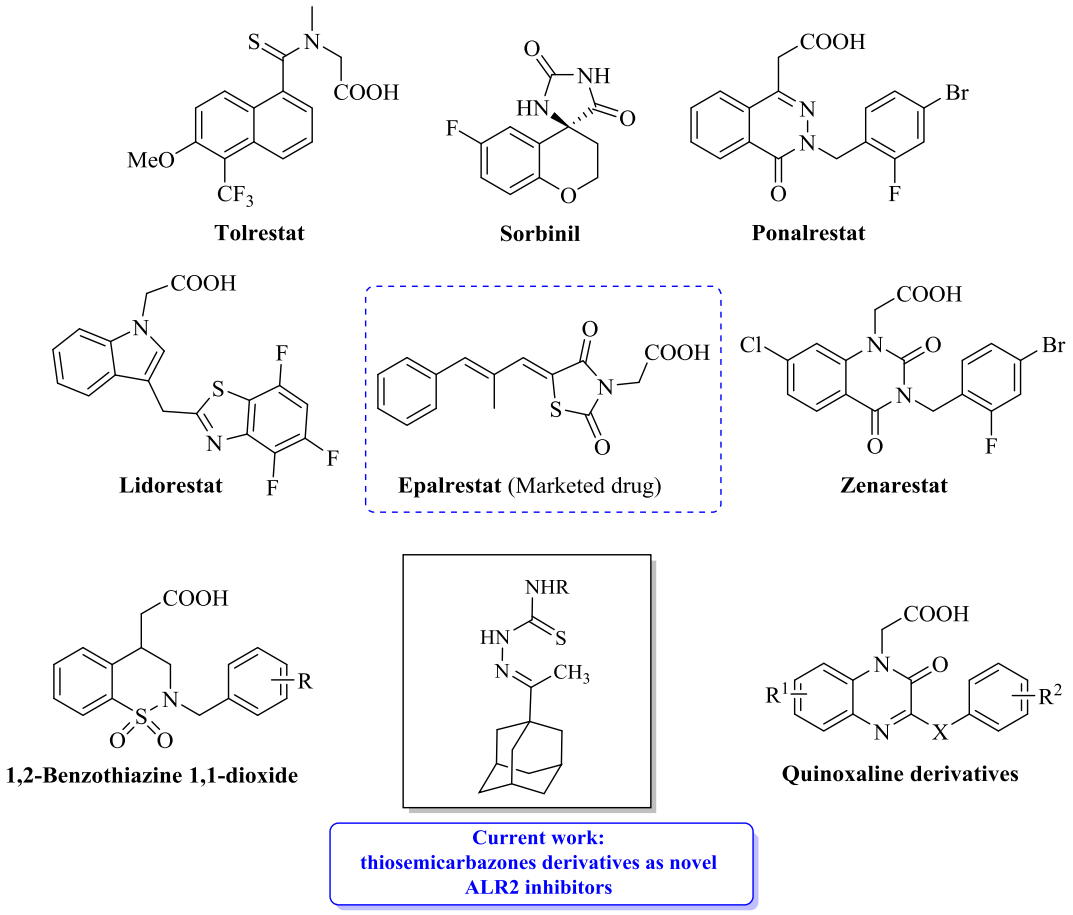

Fig. 1. Structures of some known ALR2 inhibitors and newly synthesized adamantyl-thiosemicarbazones as ALR2 inhibitor.

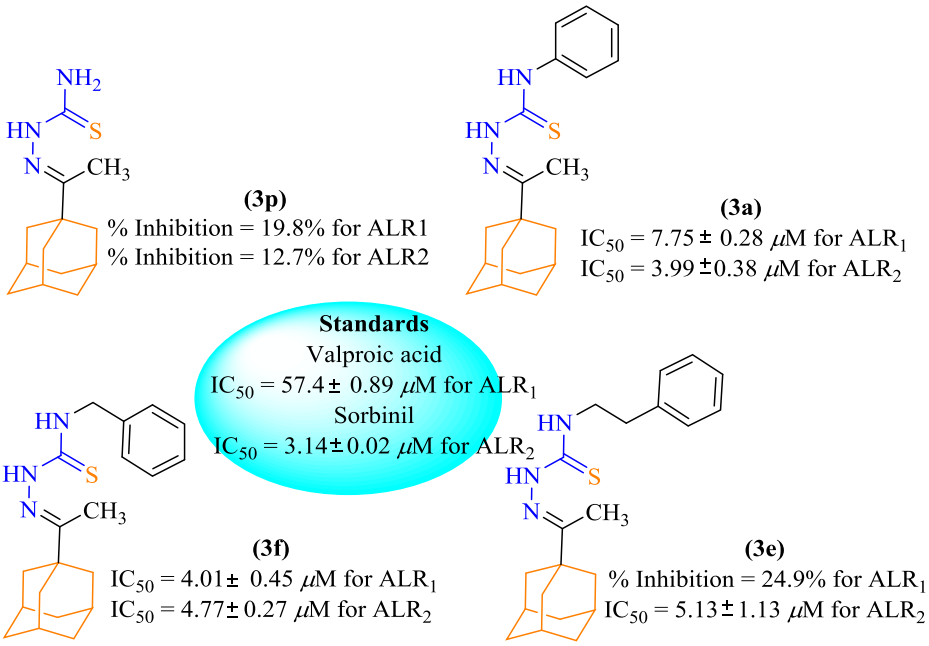

Fig. 2. ALR1 and ALR2 inhibitory activities of compounds **3p**, **3a**, **3f**, **3e**.

inhibitors is the main reason for their poor clinical profile, as quite often, these ALR2 inhibitors also simultaneously inhibit closely related ALR1 enzyme. The role of ALR1 is crucial as it is involved in the detoxification process in the liver by reducing toxic aldehydes like methylglyoxal and 3-deoxyglucosone. In addition to poor selectivity, most of the carboxylic acid and hydantoin based ALR2 inhibitors cause undesirable side effects like high toxicity and hypersensitivity [18].

Another related off-set target of ALR2 is also a member of aldo-keto reductase family 1B10 or ALKRIB10 or AKR1B10, which shares about 71% amino acid sequence identity with ALR1 (ALKR1B1 or AKR1B1)

[19]. The preferred substrate for ALKRIB10 is retinaldehyde. Interestingly, this enzyme is tumor marker for certain types of cancers, particularly the smoking related non-small cell lung carcinoma (NSCLC) [20], hence it is an prospective target for cancer treatment [20]. Whereas, it's low expression is linked to bowel diseases including gastrointestinal and colorectal cancer [21].

In continuation of our efforts to develop efficient, selective and safe pharmacophores as ALR2 inhibitors [22–30], a series of N^4-substituted thiosemicarbazone derivatives was synthesised and their potential was explored via *in vitro* inhibition studies against aldehyde and aldose reductase enzymes. The molecular docking studies were carried out to support the experimental studies, and to investigate the binding site interactions of the inhibitors in the active site of the enzyme.

2. Results and discussion

2.1. Chemistry

To investigate the biological potential of adamantyl based thiosemicarbazone, a series of adamantyl based thiosemicarbazones **(3a-p)** was synthesized by utilizing a typical condensation method by treating thiosemicarbazides (**1a-p**) with adamantyl methyl ketone (**2**). Methanol was used as solvent with glacial acetic acid as a catalyst. The optimization of reaction conditions was done by reacting equimolar quantities of phenyl thiosemicarbazide (**1a**) and adamantyl methyl ketone (**2**) in the presence of solvents of variable polarity i.e. methanol, ethanol, DMSO, DCM and THF. The optimum conditions were found by refluxing the reaction mixture in the presence of methanol as a solvent under catalysis of glacial acetic acid. The scope of reaction was broadened by using a variety of N^4-substituted thiosemicarbazides (**1a-p**). The targeted thiosemicarbazones (**3a-p**) were obtained in good to excellent yields (75–90%).

The structures of novel adamantly based thiosemicarbazones were confirmed by using spectral data IR, ^{1}H NMR, and ^{13}C NMR and microanalysis (CHN) The NH band in FTIR appeared in the range of 3245–3318 cm^{-1}, whereas C═S stretching was found between 1518 and 1599 cm^{-1} which shows the presence of new azomethine C═N linkage in thiosemicarbazones. In ^{1}H NMR, NH−N═C appeared in the range from δ 9.13–9.93 ppm while the NH−C═S showed singlet from δ 9.80–10.66 ppm. Interestingly the NH signal in NH-CH_2 bearing moieties appeared as triplet in the range from 7.79 to 8.35 (**3e, 3f, 3j and 3o**). The spectral data of all other compounds in the series confirmed the structures of desired adamantly–thiosemicarbazones **(3a-p)** (see Scheme 1).

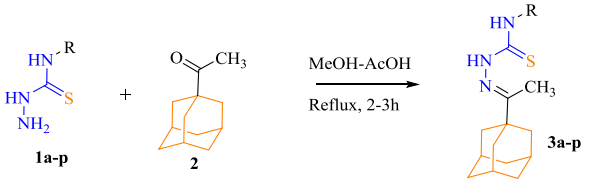

(a)	R = C_6H_5	**(i)**	R = C_6H_{11}
(b)	R = $C_{10}H_7$	**(j)**	R = 
(c)	R =4-$NO_2C_6H_4$	**(k)**	R = 3-ClC_6H_4
(d)	R =3-$OCH_3C_6H_4$	**(l)**	R = 3-BrC_6H_4
(e)	R=$C_6H_5CH_2CH_2$	**(m)**	R = 2, 6-$(CH_3)_2C_6H_3$
(f)	R= $C_6H_5CH_2$	**(n)**	R = 4-FC_6H_4
(g)	R=2-$CH_3C_6H_4$	**(o)**	R = 2-$ClC_6H_4CH_2$
(h)	R=4-$CH_3C_6H_4$	**(p)**	R = H

Scheme 1. Synthesis of adamantyl-thiosemicarbazones **(3a-p).**

Table 1
In vitro aldehyde and aldose reductase inhibitions by adamantyl-thiosemicarbazones 3a-p.

Compound No.	Structures	ALR1	ALR2
		IC_{50} ± SEM (μM)[a]/%inhibition	
3a		7.75 ± 0.28	3.99 ± 0.38
3b	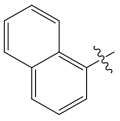	6.15 ± 0.95	5.84 ± 0.17
3c	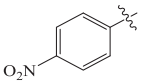	38.2 ± 1.43	5.66 ± 1.08
3d	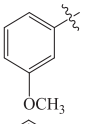	5.71 ± 0.82	7.26 ± 1.62
3e	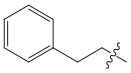	24.9%	5.13 ± 1.13
3f	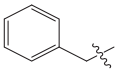	4.01 ± 0.45	4.77 ± 0.27
3g	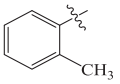	7.26 ± 0.39	3.55 ± 0.26
3h	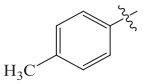	10.2%	24.8%
3i		16.4%	30.6%
3j	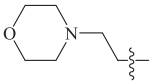	31.2%	11.6%
3k	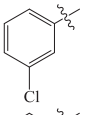	5.13 ± 0.05	38.4 ± 2.34
3l	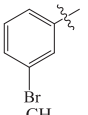	15.7 ± 0.89	33.8 ± 2.56
3m	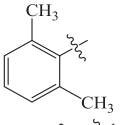	7.04 ± 2.23	1.37 ± 0.92
3n	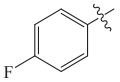	21.3%	3.48 ± 0.15
3o	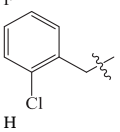	21.8%	8.67%
3p	H	19.8%	12.7%
Valproic acid [b]	–	57.4 ± 0.89	–
Sorbinil [b]	–	–	3.14 ± 0.02

[a] Half maximal inhibitory concentration.
[b] Standard inhibitor.

2.2. In vitro aldose inhibition

The adamantyl based thiosemicarbazones **(3a-p)** were screened for aldose reductase (ALR2) inhibitory activity to demonstrate their antidiabetic potential. The compounds **(3a-p)** were also screened against

aldehyde reductase enzyme (ALR1), to assess selectivity toward ALR2 over ALR1. The compound **3p** with free amino group of thiosemicarbazide moiety showed weak inhibitory activity of 12.7% for ALR2, and 19.8% inhibition for ALR1 as compared to standard sorbinil and valproic acid with IC_{50} values of 3.14 ± 0.02 µM and 57.4 ± 0.89 µM), respectively (Table 1). Furthermore, the functionalization of amino group with phenyl ring to compound **3a** showed improved inhibitory activity for ALR2 (IC_{50} = 3.99 ± 0.38 µM) as well as against ALR1 (IC_{50} = 7.75 ± 0.28 µM) enzymes. Compound **3f** bearing benzyl group, and compound **3e** with phenethyl group, showed slightly low activity with IC_{50} values of 4.77 ± 0.27 µM and 5.13 ± 1.13 µM, respectively. The compound **3f** also showed inhibitory activity against ALR1 with IC_{50} value of 4.01 ± 0.39 µM, while the compound **3e** showed weak activity with 24.9% inhibition towards ALR1 a beneficial factor towards finding lead compounds (Fig. 2).

Compound **3m,** with 2,6-dimethylphenyl substituted group, was found to be the most potent inhibitor of ALR2 with IC_{50} value of 1.37 ± 0.92 µM. Removal of one of the methyl groups, as in compound **3g,** also reduced the ALR2 inhibitory activity (IC_{50} = 3.55 ± 0.26 µM), but it was still comparable to sorbinil (IC_{50} = 3.14 ± 0.02 µM). The compounds **3m** and **3g** showed IC_{50} values of 7.04 ± 2.23 µM and 7.26 ± 0.39 µM, respectively against ALR1. The inhibitory activity of compound **3h,** containing 4-methylphenyl substituent, completely diminished for both enzymes ALR1 and ALR2 with 10.2% and 24.8% inhibition respectively. Compound **3c,** with electron withdrawing nitro group, and **3d** with electron denoting group, were also active inhibitors of ALR2 having IC_{50} values of 5.66 ± 1.08 µM and 7.26 ± 1.62 µM, respectively. However, against ALR1, the inhibitory activity of nitrophenyl substituted thiosemicarbazone **3c** (IC_{50} = 38.2 ± 1.43 µM) was much less than methoxyphenyl substituted derivative **3d** (IC_{50} = 5.71 ± 0.82 µM); this demonstrates selectivity of **3c** towards ALR2 over ALR1 (Fig. 3).

Among the halogen substituted thiosemicarbazone derivatives, the compound **3n** with 4-fluorophenyl substituent was found to be the most potent ALR2 inhibitor, with IC_{50} value of 3.48 ± 0.15 µM. Furthermore, the compound **3n** was also selective ALR2 inhibitor over ALR1, exhibiting only 21.3% inhibition against ALR1. The other halogen substituted compounds (**3k, 3l**) were weakly active against ALR2, while **3o** was not active against ALR2 (Fig. 4). The derivatives bearing naphthalene **3b**, cyclohexyl **3i**, and morpholinoethyl **3j** substituents showed activity with IC_{50} value of 3.48 ± 0.15 µM, 30.6% and 11.6% percentage inhibition, respectively, for ALR2 and 6.15 ± 0.95 µM, 16.4% and 31.2% percentage inhibition, respectively, for ALR1 (Fig. 5).

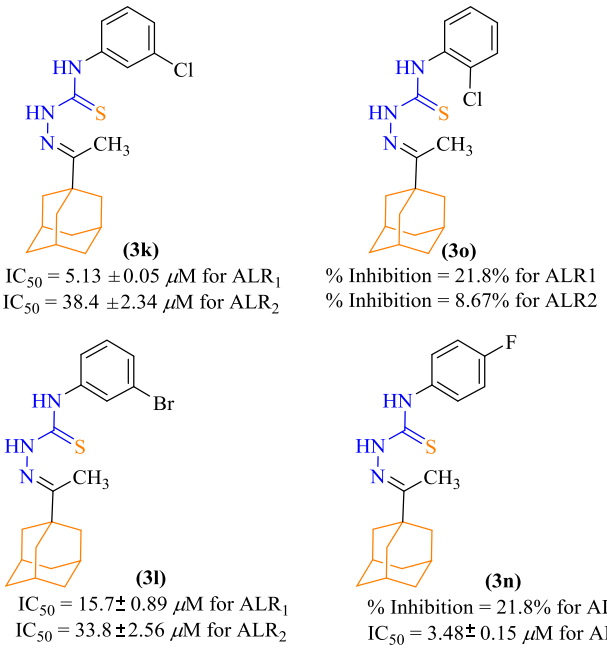

Fig. 4. ALR1/ALR2 inhibitory activities of halogen substituted compounds **3k, 3o, 3l** and **3n**.

2.3. Docking results

Since crystal structure of human ALR1 is not available from the

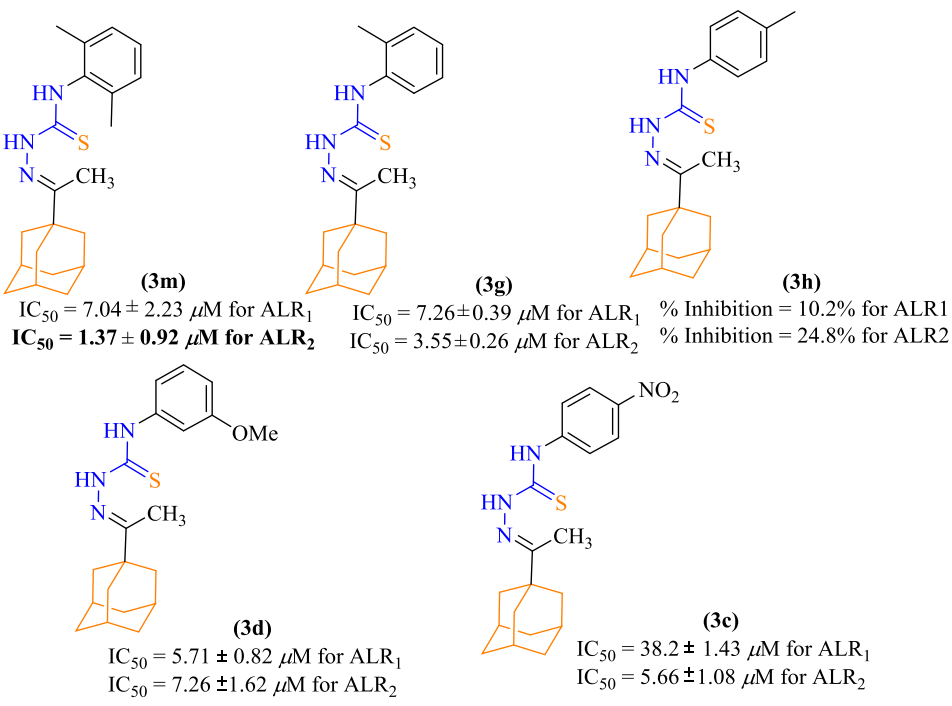

Fig. 3. ALR2 activity of methyl (**3m, 3g, 3h**), methoxy (**3d**) and nitro (**3c**) derivatives.

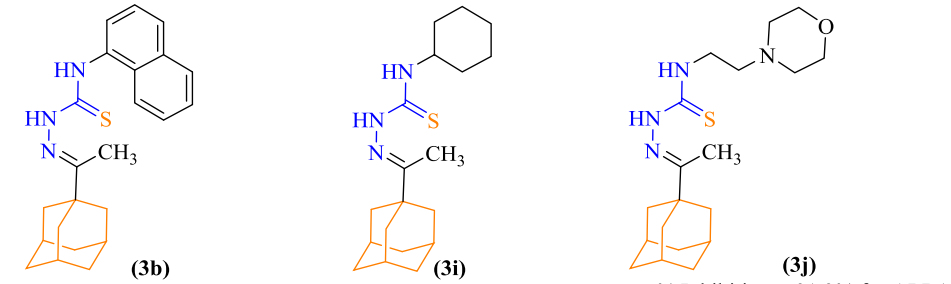

Fig. 5. Bioactivity of naphthalene **3b**, cyclohexyl **3i** and morpholinoethyl **3j** linked derivatives.

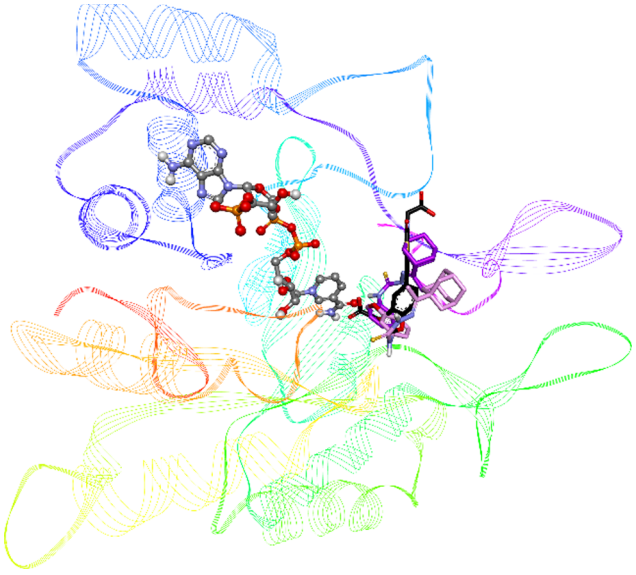

Fig. 6. An overlap of docked conformations of active ALR1 inhibitors **3d** (pink) and **3f** (purple) with the co-crystallized inhibitor [5-(3-carboxymethoxy-4-methoxybenzylidene)-2,4-dioxothiazolidin-3-yl]acetic acid (FX4, black), the co-factor NADP is shown in ball and stick representation.

PDB, therefore crystal structure of porcine ALR1 was downloaded (PDB id: 3FX4, 1.99 Å) and used for the docking studies, as previously reported [31]. Molecular docking was performed with active admentyl-thiosemcarbazones ALR1 inhibitors (**3d** and **3f**) which showed binding at the same place of active site as that of co-crystallized inhibitor FX4 ([5-(3-carboxymethoxy-4-methoxybenzylidene)-2,4-dioxothiazolidin-3-yl]acetic acid). Fig. 6 shows overlap of predicted docked conformation of **3d** (pink) and **3f** (purple) with FX4 (black), the co-factor NADP is shown in ball and stick representation.

Fig. 7 shows predicted 3D and 2D binding interactions of compound **3d** within the active site of ALR1. The NH group of thiourea moiety formed hydrogen bond with the carbonyl group of Ile49. A π-sulfur interaction was observed between thiocarbonyl group and Trp22. The π -Alkyl interactions were observed between the phenyl ring of 3d with Ile49, and between the adamantyl group and Phe125.

For compound **3f**, the NH group of thiourea moiety was found to be making a hydrogen bond with the enzyme co-factor NADP. Moreover, π -sulfur interactions were observed between the thiocarbonyl group and Trp114. The adamantyl group was making pi-alkyl interactions with Trp22 and Ala219 (Fig. 8).

Docking studies were also carried out for compounds **3m** and **3n**, which exhibited maximum inhibitory potential towards ALR2. For ALR2 docking, the crystal structure of human ALR2 in complex with an inhibitor was downloaded from the Protein Data Bank (PDB id: 1US0, 0.66 Å). The both thiosemcarbazones **3m** and **3n** showed binding with the active site of target enzyme at the same place as that of co-crystallized inhibitor LDT ([2-(4-bromo-2-fluoro-benzylthiocarbamoyl)-5-fluoro-phenoxy]-acetic acid), as can be seen in Fig. 9.

Docked conformation of **3m** is shown in Fig. 10. An extensive network of π - π stacked and π -alkyl interactions was observed. The adamantyl group was formed π -alkyl interactions with Pro218 and Phe122. From two methyl groups, one substituted methyl groups on phenyl ring formed π -alkyl interactions with Phe122, Trp79, and Trp111. While the other methyl group formed π -alkyl interactions with Tyr309, Cys303 and Leu300. The phenyl ring also developed π -alkyl interaction with Leu300 and Cys303. Further, the same phenyl ring formed π - π *T*-shaped interaction with Phe122. With Trp111, π - π stacked interaction with the phenyl ring was also observed.

For compound **3n**, similar interactions were observed (Fig. 11). The adamantyl group was making π -alkyl interactions with Trp20 and Pro218. The thiocarbonyl group also developed π -sulfur interactions with Trp79 and Phe122. Moreover, another π -sulfur interaction was observed between the phenyl ring of compound **3n** and Cys80. The same phenyl ring was also making π -alkyl interaction with Leu300, and π - π stacked interaction with Trp111.

3. Conclusions

To pursue our interest in thisosemicarbazones as selective ALR2 inhibitors, herein, we have studied the ALR1 and ALR2 inhibitory potential of newly synthesized adamantyl thiosemicarbazones **(3a-p)**. Most of the compounds showed good inhibitory activity against ALR2 with IC_{50} values ranging between 1.37 ± 0.92 to 38.4 ± 2.34 μM. The thiosemicarbazones having phenyl (**3a)**, 2,6-dimethylphenyl (**3m)** and 2-methylphenyl (**3g)** substituents were found to be most potent ALR2 inhibitors with IC_{50} values of 3.99 ± 0.38, 1.37 ± 0.92, 3.55 ± 0.26 μM, respectively, as compared with IC_{50} value of 3.14 ± 0.02 μM reference inhibitor, sorbinil. Moreover, molecular docking studies have also been performed to rationalize binding site interactions of adamantyl-thiosemicarbazones. The lead compounds (**3a**, **3m**, and **3g**) identified in this study can potentially be used to develop new therapeutic agents.

4. Experimental work

4.1. Materials and methods

The starting materials which include 1-Adamantyl methyl ketone (Sigma-Alrich ≥ 99%) and other required chemicals were purchased from different commercial sources and used without purification unless otherwise stated. Ethanol, glacial acetic acid (Sigma-Alrich ≥ 99.85%) and other solvents were also purchased and used without purification in the reaction media. Distilled water was used for reaction workup purpose as solvent. The progress of reactions was monitored by using thin layer chromatography (TLC) with silica gel 60 aluminium-backed plates

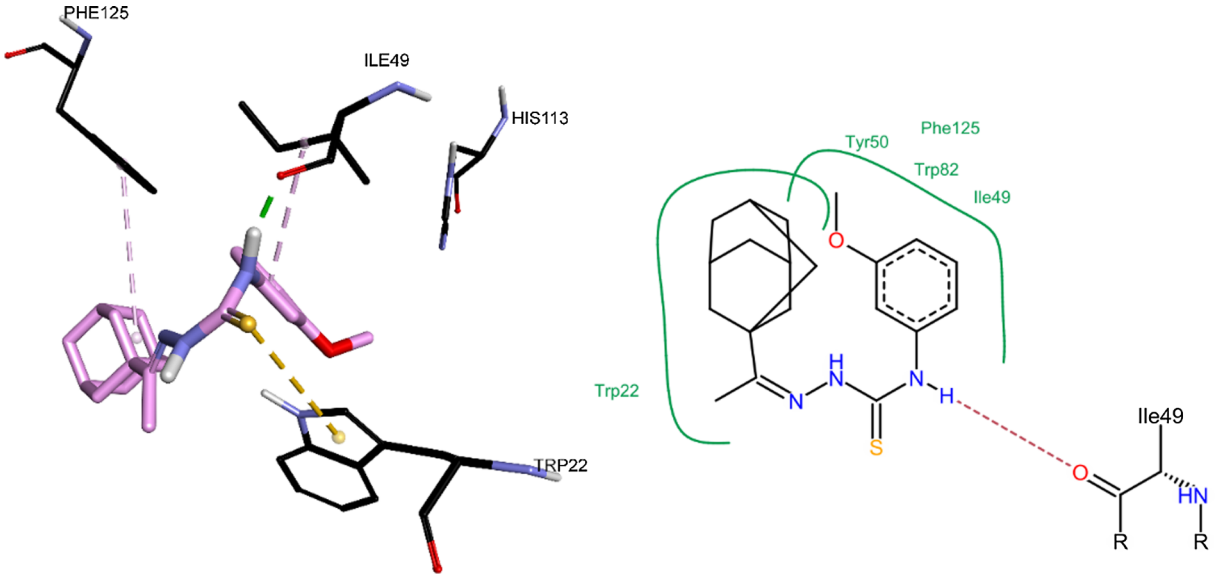

Fig. 7. 3D and 2D interactions of docked conformation of 3d within active site of ALR1.

0.063–0.200 mm The Infrared spectra IR (KBr discs) were recorded in the range 4000–500 cm^{-1} *via* Bruker Vector-22 spectrometer and the ^1H NMR spectra were recorded *via* Bruker spectrometer 400 MHz as dilute solutions in suitable deuterated solvent at 25 °C. The chemical shifts were recorded on the *δ*-scale (ppm) using residual solvents as an internal standard (DMSO; ^1H 2.50, and $CHCl_3$; ^1H 7.26,). Coupling constant were calculated in Hertz (Hz) and multiplicities were labelled as s (singlet), d (doublet), t (triplet), q (quartet), quint (quintet) and the prefixes br (broad) or app (apparent) were used. Melting points of synthesized compounds were determined by means of a Stuart™ melting point SMP3 apparatus.

4.2. Chemistry

4.2.1. General procedure for the synthesis of compounds (3a-p)

The adamantyl based thiosemicarbazones (**3a-p**) were prepared by following general procedure. In a typical procedure by using the optimized conditions, the corresponding N^4-substituted thiosemicarbazides (1.0 mmol, 1.0 equiv.) was placed in an oven dried round bottomed flask along with adamantyl methyl ketone (**2**) (1.0 mmol, 1.0 equiv.) and methanol (4–5 mL) to solubilize the reactants. In this reaction mixture, glacial acetic acid was added as catalyst and then resulting mixture was heated at reflux until the complete consumption of starting materials, monitored by TLC analysis. The compounds were purified by crystallization from ethanol or by using silica gel column chromatography with eluents ethyl acetate/hexane in gradients elution (0:1–1:0) to obtained the desired thiosemicarbazones (**3a-p**) in good to excellent yields (**75–90%**).

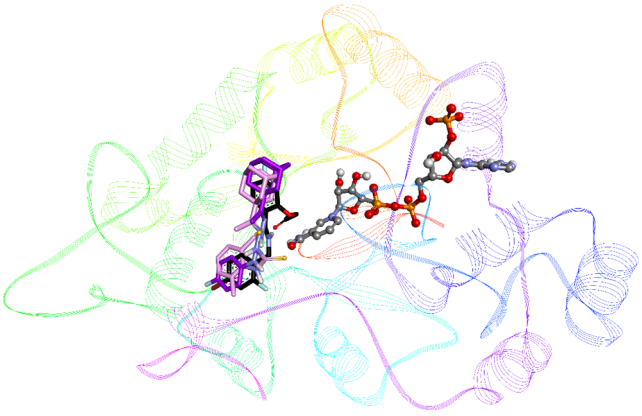

Fig. 9. An overlap of docked conformations of most active ALR2 inhibitors **3m** (pink) and **3n** (purple) with the co-crystallized inhibitor ([2-(4-bromo-2-fluoro-benzylthiocarbamoyl)-5-fluoro-phenoxy]-acetic acid (LDT, black), the co-factor NADP is shown in ball and stick representation.

4.2.1.1. (2-(1-(Adamantan-1-yl)ethylidene)-N-phenylhydrazinecarbothioamide (3a).

Yield 80%, m.p. 166–168 °C, IR υ_{max} (cm^{-1}): 1182(C═S), 1587(C═N), 3148, 3300 (N−H); ^1H NMR

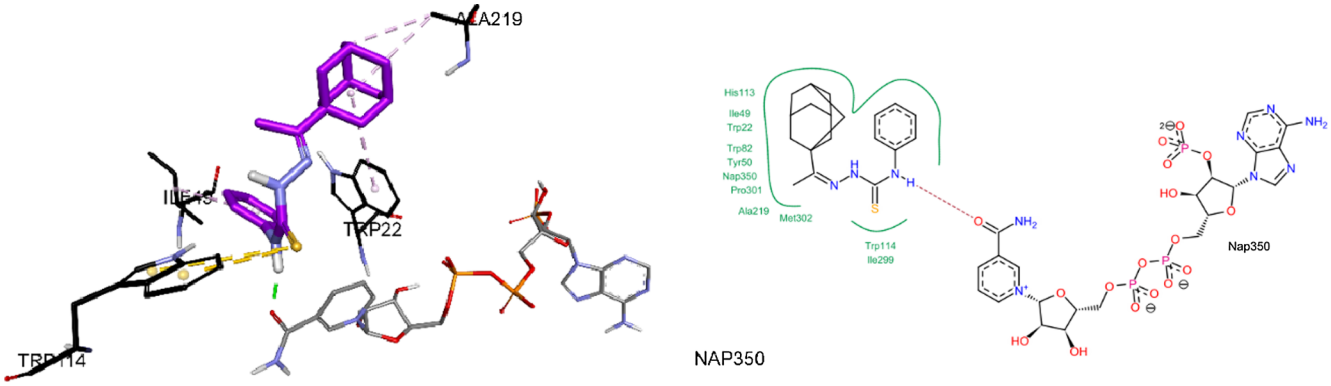

Fig. 8. 3D and 2D interactions of docked conformation of **3f** within active site of ALR1.

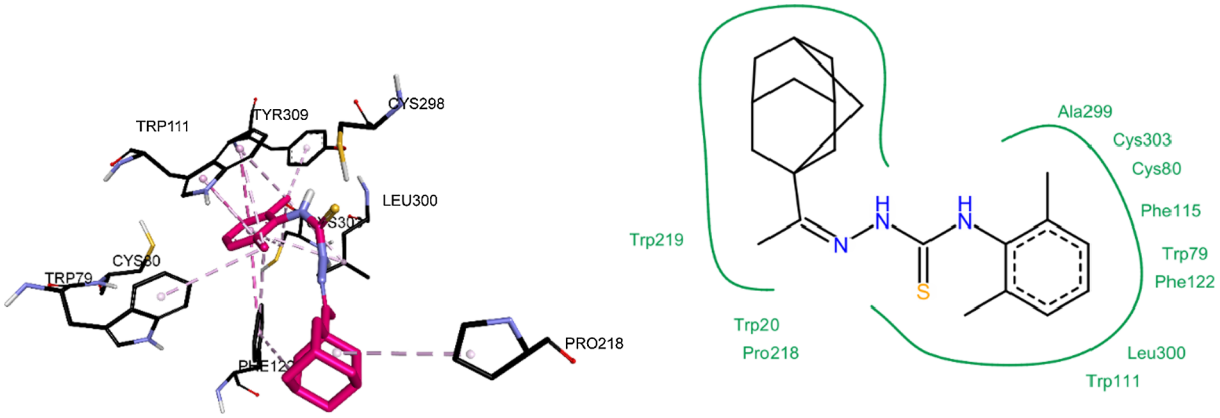

Fig. 10. 3D and 2D interactions of docked conformation of **3m** within active site of ALR2.

(DMSO-d_6) δ ppm; 1.61–1.63 (bd, 6H, adamantane $-CH_2$), 1.72–1.73 (bd, 6H, adamantane $-CH_2$), 1.87 (s, 3H, CH_3), 1.95–1.96 (bd, 3H, adamantane $-CH_2$), 7.13 (m, 1H), 7.3 (dd, 2H, J = 7.6, 0.8 Hz), 7.55 (dd, 2H, J = 7.6, 1.6 Hz), 9.54 (s, 1H, NH), 10.25 (s, 1H, NH); ^{13}C NMR δ ppm; 12.58, 28.15, 36.68, 39.23, 40.69, 125.09, 128.71, 128.74, 139.35, 161.20, 177.06; Anal calcd for $C_{19}H_{25}N_3S$ (327.49); C, 69.68; H, 7.69; N, 12.83; Found; C, 69.60; H, 7.58; N, 12.72.

*4.2.1.2. 2-(1-(Adamantan-1-yl)ethylidene)-N-(naphthalen-1-yl) hydrazinecarbothioamide (**3b**).* Yield 76%, m.p.210–212 °C, IR υ_{max} (cm^{-1}): 1195 (C═S), 1597 (C═N), 3148, 3303 (N−H); ^{1}H NMR (DMSO-d_6) δ ppm; 1.61–1.63 (bd, 6H, adamantane $-CH_2$), 1.76–1.77 (bd, 6H, adamantane $-CH_2$), 1.93 (s, 3H, CH_3), 1.95–1.96 (bd, 3H, adamantane $-CH_2$), 7.48–7.66 (m, 3H), 7.79–7.83 (m, 2H), 7.92–7.97 (m, 2H), 9.83 (s, 1H, NH), 10.37 (s, 1H, NH); ^{13}C NMR δ ppm; 12.64, 28.18, 36.72, 39.37, 40.70, 125.09, 122.97, 125.79, 125.90, 126.55, 126.76, 126.96, 128.72, 130.31, 134.18, 135.70, 161.26, 179.90; Anal calcd for $C_{23}H_{27}N_3S$ (377.55); C, 73.17; H, 7.21; N, 11.13 Found; C, 73.10; H, 7.25; N, 11.22.

*4.2.1.3. 2-(1-(Adamantan-1-yl)ethylidene)-N-(4-nitrophenyl) hydrazinecarbothioamide (**3c**).* Yield 82%, m.p. 176–177 °C, IR υ_{max} (cm^{-1}): 1169 (C═S), 1599 (C═N), 3240, 3318 (N−H); ^{1}H NMR (DMSO-d_6) δ ppm; 1.59–1.63 (bd, 6H, adamantane $-CH_2$), 1.73–1.74 (bd, 6H, adamantane $-CH_2$), 1.89 (s, 3H, CH_3), 1.96–1.97 (bd, 3H, adamantane $-CH_2$), 8.01 (dd, 2H, J = 7.2, 2.4 Hz), 8.17 (dd, 2H, J = 7.2, 2.4 Hz), 9.93 (s, 1H, NH), 10.66 (s, 1H, NH); ^{13}C NMR δ ppm; 12.84, 28.13, 36.70, 39.11, 40.83, 123.65, 124.47, 144.74, 145.68, 162.78, 176.48; Anal calcd for $C_{19}H_{24}N_4O_2S$ (372.48); C, 61.27; H, 6.49; N, 15.04 Found; C, 61.42; H, 6.60; N, 15.11

*4.2.1.4. (2-(1-(Adamantan-1-yl)ethylidene)-N-(3-methoxyphenyl) hydrazinecarbothioamide (**3d**).* Yield 80%, m.p. 122–124 °C, IR υ_{max} (cm^{-1}): 1169 (C═S), 1592 (C═N), 3245 (N−H); ^{1}H NMR (DMSO-d_6) δ ppm; 1.62–1.63 (bd, 6H, adamantane $-CH_2$), 1.71–1.72 (bd, 6H, adamantane $-CH_2$), 1.87 (s, 3H, CH_3), 1.96–1.97 (bd, 3H, adamantane $-CH_2$), 3.87 (s, 3H, OCH_3), 6.72–6.96 (m, 1H), 7.03–7.06 (m, 1H), 7.20 (t, 1H, J = 8.0 Hz), 7.37 (t, 1H, J = 2.8 Hz), 9.52 (s, 1H, NH), 10.25 (s, 1H, NH); ^{13}C NMR δ ppm; 12.59, 28.14, 36.68, 39.21, 40.70, 55.67, 110.49, 110.85, 117.01, 129.51, 140.44, 159.61, 161.26, 176.99; Anal calcd for $C_{20}H_{27}N_3OS$ (357.51); C, 67.19; H, 7.61; N, 11.75 Found; C, 67.28; H, 7.58; N, 11.92

*4.2.1.5. 2-(1-(Adamantan-1-yl)ethylidene)-N-phenethylhydrazinecarbothioamide (**3e**).* Yield 84%, m.p. 150–152 °C, IR υ_{max} (cm^{-1}): 1182 (C═S), 1524 (C═N), 3312 (N−H), ^{1}H NMR (DMSO-d_6) δ ppm; 1.57–1.63 (bd, 12H, adamantane $-CH_2$), 1.77 (s, 3H, CH_3), 1.91–1.93 (bd, 3H, adamantane $-CH_2$), 2.82 (t, 2H, J = 7.2 Hz, $-CH_2$–Ar), 2.82 (q, 2H, J = 6.0 Hz, $-CH_2$–NH), 7.17–7.26 (m, 5H), 7.79 (t, 1H, NH), 9.85 (s, 1H, −NH); ^{13}C NMR δ ppm; 12.16, 28.11, 35.12, 36.71, 39.30, 39.81, 40.48, 45.10, 126.75, 128.96, 129.20, 139.63, 159.72, 178.47; Anal calcd for $C_{21}H_{29}N_3S$ (355.54); C, 70.94; H, 8.22; N, 11.82 Found; C, 70.82; H, 8.24; N, 11.94.

*4.2.1.6. 2-(1-(Adamantan-1-yl)ethylidene)-N-benzylhydrazinecarbothioamide (**3f**).* Yield 78%, m.p. 168–170 °C, IR υ_{max} (cm^{-1}): 1183 (C═S), 1530 (C═N), 3201, 3343 (N−H); ^{1}H NMR (DMSO-d_6) δ ppm; 1.57–1.62 (bd, 6H, adamantane $-CH_2$), 1.65–1.67 (bd, 6H, adamantane $-CH_2$), 1.81 (s, 3H, CH_3), 1.93 (bd, 3H, adamantane $-CH_2$), 4.78 (d, 2H, J = 6.4 Hz, $-CH_2$–NH), 7.18–7.21

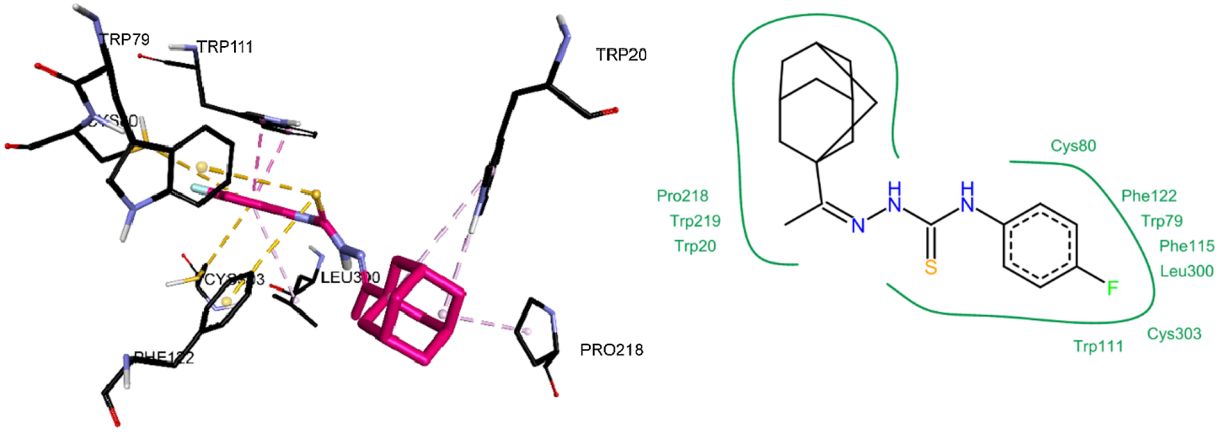

Fig. 11. 3D and 2D interactions of docked conformation of **3n** within active site of ALR2.

(m, 4H), 7.28–7.29 (m, 1H), 8.35 (t, 1H, J = 6.4 Hz, −NH), 9.88 (s, 1H, NH); ^{13}C NMR δ ppm; 12.29, 28.12, 36.70, 39.33, 39.77, 40.52, 47.10, 127.26, 128.71, 128.75, 139.97, 160.31, 179.12; Anal calcd for $C_{20}H_{27}N_3S$ (341.51); C, 70.34; H, 7.97; N, 12.30 Found; C, 70.22; H, 7.85; N, 12.45.

*4.2.1.7. 2-(1-(Adamantan-1-yl)ethylidene)-N-(2-methylphenyl) hydrazinecarbothioamide (**3g**)*. Yield 75%, m.p. 202–204 °C, IR υ_{max} (cm^{-1}): 1182 (C═S), 1518 (C═N), 3302 (N−H); ^{1}H NMR (DMSO-d_6) δ ppm; 1.62–1.63 (bd, 6H, adamantane −CH$_2$), 1.72–1.73 (bd, 6H, adamantane −CH$_2$), 1.87 (s, 3H, CH$_3$), 1.95–1.96 (bd, 3H, adamantane −CH$_2$), 2.17 (s, 3H, CH$_3$), 7.10–7.12 (m, 1H), 7.19–7.21 (m, 2H), 7.56 (dd, 1H, J = 8.4, 1.2 Hz), 9.40 (s, 1H, NH), 10.21 (s, 1H, NH); ^{13}C NMR δ ppm; 12.55, 18.25, 28.15, 36.70, 39.32, 40.65, 126.28, 126.44, 127.45, 130.54, 133.83, 138.21, 160.84, 177.65; Anal calcd for $C_{20}H_{27}N_3S$ (341.51); C, 70.34; H, 7.97; N, 12.30 Found; C, 70.42; H, 7.82; N, 12.48.

*4.2.1.8. 2-(1-(Adamantan-1-yl)ethylidene)-N-(4-methylphenyl) hydrazinecarbothioamide (**3h**)*. Yield 81%, m.p.180–182 °C, IR υ_{max} (cm^{-1}): 1197 (C═S), 1530 (C═N), 3119, 3166, 3315 (N−H); ^{1}H NMR (DMSO-d_6) δ ppm; 1.59–1.62 (bd, 6H, adamantane −CH$_2$), 1.71–1.72 (bd, 6H, adamantane −CH$_2$), 1.87 (s, 3H, CH$_3$), 1.95–1.96 (bd, 3H, adamantane −CH$_2$), 2.25 (s, 3H, CH$_3$), 7.09 (d, 2H, J = 8.8 Hz), 7.41 (d, 2H, J = 8.8 Hz), 9.46 (s, 1H, NH), 10.18 (s, 1H, NH); ^{13}C NMR δ ppm; 12.55, 21.08, 28.15, 36.69, 39.24, 40.66, 125.09, 129.09, 134.751, 136.81, 161.01, 177.12; Anal calcd for $C_{20}H_{27}N_3S$ (341.51); C, 70.34; H, 7.97; N, 12.30 Found; C, 70.45; H, 7.88; N, 12.42.

*4.2.1.9. 2-(1-(Adamantan-1-yl)ethylidene)-N-cyclohexylhydrazinecarbothioamide (**3i**)*. Yield 85%, m.p.230–232 °C, IR υ_{max} (cm^{-1}): 1182 (C═S), 1560 (C═N), 3134, 3241 (N−H); ^{1}H NMR (DMSO-d_6) δ ppm; 1.15–1.26 (m, 10H), 1.58–1.65 (bd, 6H, adamantane −CH$_2$), 1.71–1.75 (bd, 6H, adamantane −CH$_2$), 1.79 (s, 3H, CH$_3$), 1.95–1.96 (bd, 3H, adamantane −CH$_2$), 3.28 (m, 1H), 9.13 (s, 1H, NH), 9.80 (s, 1H, NH); ^{13}C NMR δ ppm; 12.24, 28.14, 31.91, 32.01, 32.67, 36.67, 39.26, 40.63, 53.19, 159.50, 177.86; Anal calcd for $C_{19}H_{31}N_3S$ (333.53); C, 68.42; H, 9.37; N, 12.60 Found; C, 68.55; H, 9.46; N, 12.75.

*4.2.1.10. 2-(1-(Adamantan-1-yl)ethylidene)-N-(2-morpholinoethyl) hydrazinecarbothioamide (**3j**)*. Yield 82%, m.p.156–158 °C, IR υ_{max} (cm^{-1}): 1202 (C═S), 1527 (C═N), 3226, 3309 (N−H); ^{1}H NMR (DMSO-d_6) δ ppm; 1.57–1.61 (bd, 6H, adamantane −CH$_2$), 1.65–1.69 (bd, 6H, adamantane −CH$_2$), 1.79 (s, 3H, CH$_3$), 1.95–1.96 (bd, 3H, adamantane −CH$_2$), 2.36 (bs, 2H, CH$_2$−N), 2.43–2.47 (m, 2H, CH$_2$−NH−C═S), 3.51–3.56 (m, 8H, −CH$_2$−CH$_2$− morpholine), 8.14 (t, 1H, NH), 9.93 (s, 1H, NH); ^{13}C NMR δ ppm; 12.10, 28.17, 36.73, 39.59, 39.78, 39.99, 40.59, 53.41, 56.44, 66.76, 159.29, 178.20; Anal calcd for $C_{19}H_{32}N_4OS$ (364.55); C, 62.60; H, 8.85; N, 15.37; Found; C, 62.50; H, 8.92; N, 15.54.

*4.2.1.11. 2-(1-(Adamantan-1-yl)ethylidene)-N-(3-chlorophenyl) hydrazinecarbothioamide (**3k**)*. Yield 78%, m.p.158–160 °C, IR υ_{max} (cm^{-1}): 1188 (C═S), 1583 (C═N), 3267, 3321 (N−H); ^{1}H NMR (DMSO-d_6) δ ppm; 1.59–1.63 (bd, 6H, adamantane −CH$_2$), 1.72–1.73 (bd, 6H, adamantane −CH$_2$), 1.87 (s, 3H, CH$_3$), 1.95–1.96 (bd, 3H, adamantane −CH$_2$), 7.32 (t, 1H, J = 8.0 Hz), 7.46–7.49 (m, 2H), 7.81 (t, 1H, J = 2.4 Hz), 9.60 (s, 1H, NH), 10.36 (s, 1H, NH); ^{13}C NMR δ ppm; 12.60, 28.14, 36.69, 39.19, 40.73, 123.76, 124.52, 125.22, 130.24, 132.78, 140.90, 161.90, 176.99; Anal calcd for $C_{19}H_{24}ClN_3S$ (361.93); C, 63.05; H, 6.68; N, 11.61; Found; C, 63.25; H, 6.75; N, 11.50.

*4.2.1.12. 2-(1-(Adamantan-1-yl)ethylidene)-N-(3-bromophenyl) hydrazinecarbothioamide (**3l**)*. Yield 90%, m.p.178–180 °C, IR υ_{max} (cm^{-1}): 1201 (C═S), 1572 (C═N), 3324 (N−H); ^{1}H NMR (DMSO-d_6) δ ppm; 1.59–1.63 (bd, 6H, adamantane −CH$_2$), 1.72–1.75 (bd, 6H, adamantane −CH$_2$), 1.87 (s, 3H, CH$_3$), 1.96–1.97 (bd, 3H, adamantane −CH$_2$), 7.23–7.33 (m, 2H), 7.521 (dd, 1H, J = 8.0, 1.2 Hz), 7.93 (t, 1H, J = 2.4 Hz), 9.59 (s, 1H, NH), 10.36 (s, 1H, NH); ^{13}C NMR δ ppm; 12.68, 28.15, 36.69, 39.19, 40.73, 1231.31, 124.28, 127.41, 128.12, 130.51, 141.06, 161.91, 177.02; Anal calcd for $C_{19}H_{24}BrN_3S$ (406.38); C, 56.15; H, 5.95; N, 10.34; Found; C, 56.05; H, 5.80; N, 10.42.

*4.2.1.13. 2-(1-(Adamantan-1-yl)ethylidene)-N-(2,6-dimethylphenyl) hydrazinecarbothioamide(**3m**)*. Yield 88%, m.p.261–263 °C, IR υ_{max} (cm^{-1}): 1189 (C═S), 1545 (C═N), 3301 (N−H); ^{1}H NMR (DMSO-d_6) δ ppm; 1.61–1.63 (bd, 6H, adamantane −CH$_2$), 1.72–1.75 (bd, 6H, adamantane −CH$_2$), 1.89 (s, 3H, CH$_3$), 1.95–1.96 (bd, 3H, adamantane −CH$_2$), 2.17 (s, 6H, CH$_3$), 7.10–7.12 (dd, 2H, J = 8.0, 1.2 Hz), 7.35 (dd, 1H, J = 8.0 Hz), 9.45 (s, 1H, NH), 10.20 (s, 1H, NH); ^{13}C NMR δ ppm; 12.56, 18.25, 28.17, 36.73, 39.36, 40.55, 126.18, 126.54, 127.15, 130.33, 160.44, 177.61; Anal calcd for $C_{21}H_{29}N_3S$ (355.54); C, 70.94; H, 8.22; N, 11.82; Found; C, 70.85; H, 8.34; N, 11.95.

*4.2.1.14. 2-(1-(Adamantan-1-yl)ethylidene)-N-(4-fluorophenyl) hydrazinecarbothioamide (**3n**)*. Yield 78%, m.p.168–170 °C, IR υ_{max} (cm^{-1}): 1171 (C═S), 1543 (C═N), 3253, 3372 (N−H); ^{1}H NMR (DMSO-d_6) δ ppm; 1.58–1.63 (bd, 6H, adamantane −CH$_2$), 1.72–1.73 (bd, 6H, adamantane −CH$_2$), 1.96–1.97 (bd, 3H, adamantane −CH$_2$), 1.97 (s, 3H, CH$_3$), 7.13 (dd, 2H, J = 8.8, 2.0 Hz), 7.50 (dd, 2H, J = 7.6, 2.4 Hz), 9.50 (s, 1H, NH), 10.24 (s, 1H, NH); ^{13}C NMR δ ppm; 12.57, 28.12, 36.70, 39.24, 40.68, 115.39, 127.79, 135.82, 137.14, 161.36, 177.57; Anal calcd for $C_{19}H_{24}FN_3S$ (345.48); C, 66.05; H, 7.00; N, 12.16 Found; C, 66.21; H, 7.14; N, 12.30.

*4.2.1.15. 2-(1-(Adamantan-1-yl)ethylidene)-N-(2-chlorobenzyl) hydrazinecarbothioamide (**3o**)*. Yield 75%, m.p.218–20 °C, IR υ_{max} (cm^{-1}): 1181 (C═S), 1526 (C═N), 3185, 3332 (N−H); ^{1}H NMR (DMSO-d_6) δ ppm; 1.61–1.63 (bd, 6H, adamantane −CH$_2$), 1.69–1.70 (bd, 6H, adamantane −CH$_2$), 1.83 (s, 3H, CH$_3$), 1.94 (bd, 3H, adamantane −CH$_2$), 4.83 (d, 2H, J = 6.8 Hz, −CH$_2$−NH), 7.22–7.29 (m, 2H), 7.39–7.42 (m, 2H), 8.43 (t, 1H, J = 6.8 Hz, −NH), 10.04 (s, 1H, NH); ^{13}C NMR δ ppm; 12.34, 28.19, 36.71, 39.28, 39.92, 40.18, 45.15, 127.58, 128.98, 129.58, 132.17, 136.89, 160.61, 179.39; Anal calcd for $C_{20}H_{26}ClN_3S$ (375.96); C, 63.89; H, 6.97; N, 11.18 Found; C, 63.75; H, 6.79; N, 11.30.

*4.2.1.16. 2-(1-(Adamantan-1-yl)ethylidene)hydrazinecarbothioamide (**3p**)*. Yield 85%, m.p.210–212 °C, IR υ_{max} (cm^{-1}): 1185 (C═S), 1589 (C═N), 3126, 3408 (N−H); ^{1}H NMR (DMSO-d_6) δ ppm; 1.56–1.62 (bd, 6H, adamantane −CH$_2$), 1.65–1.70 (bd, 6H, adamantane −CH$_2$), 1.79 (s, 3H, CH$_3$), 1.93–1.94 (bd, 3H, adamantane −CH$_2$), 8.07 (s, 1H, NH), 9.80 (s, 2H, NH); ^{13}C NMR δ ppm; 12.15, 28.12, 36.72, 39.39, 40.50, 160.04, 179.28; Anal calcd for $C_{13}H_{21}N_3S$ (251.39); C, 62.11; H, 8.42; N, 16.72 Found; C, 62.25; H, 8.31; N, 16.84.

Acknowledgement

J. Iqbal is thankful to the Organization for the Prohibition of Chemical Weapons (OPCW), The Hague, The Netherlands and Higher Education Commission of Pakistan through Project No. 20-3733/NRPU/R&D/14/520 for the financial support. Z. Shafiq is thankful to Higher Education Commission of Pakistan for financial support vide Project No. NRPU-I/6975.

Appendix A. Supplementary material

Supplementary data to this article can be found online at https://doi.org/10.1016/j.bioorg.2019.103244.

References

[1] R. Ottanà, R. Maccari, M. Giglio, A. Del Corso, M. Cappiello, U. Mura, S. Cosconati, L. Marinelli, E. Novellino, S. Sartini, C. La Motta, F. Da Settimo, Identification of 5-arylidene-4-thiazolidinone derivatives endowed with dual activity as aldose reductase inhibitors and antioxidant agents for the treatment of diabetic complications, Eur. J. Med. Chem. 46 (2011) 2797–2806.

[2] Y. Shi, F.B. Hu, The global implications of diabetes and cancer, The Lancet 383 (2014) 1947–1948.

[3] D.R. Whiting, L. Guariguata, C. Weil, J. Shaw, IDF diabetes atlas: global estimates of the prevalence of diabetes for 2011 and 2030, Diabetes Res. Clin. Pract. 94 (2011) 311–321.

[4] S. Ovais, H. Pushpalatha, G.B. Reddy, P. Rathore, R. Bashir, S. Yaseen, A. Dheyaa, R. Yaseen, O. Tanwar, M. Akthar, Synthesis and biological evaluation of some new pyrazoline substituted benzenesulfonylurea/thiourea derivatives as anti-hyperglycaemic agents and aldose reductase inhibitors, Eur. J. Med. Chem. 80 (2014) 209–217.

[5] M. Brownlee, Biochemistry and molecular cell biology of diabetic complications, Nature 414 (2001) 813.

[6] J.H. Kinoshita, C. Nishimura, The involvement of aldose reductase in diabetic complications, Diabetes Metab. Rev. 4 (1988) 323–337.

[7] R. Maccari, R. Ottanà, Targeting aldose reductase for the treatment of diabetes complications and inflammatory diseases: new insights and future directions, J. Med. Chem. 58 (2014) 2047–2067.

[8] M. Chatzopoulou, K. Pegklidou, N. Papastavrou, V.J. Demopoulos, Development of aldose reductase inhibitors for the treatment of inflammatory disorders, Expert Opin. Drug Discov. 8 (2013) 1365–1380.

[9] A. Bhatnagar, S.K. Srivastava, Aldose reductase: congenial and injurious profiles of an enigmatic enzyme, Biochem. Med. Metab. Biol. 48 (1992) 91–121.

[10] O. El-Kabbani, V. Carbone, C. Darmanin, M. Oka, A. Mitschler, A. Podjarny, C. Schulze-Briese, R.P.-T. Chung, Structure of aldehyde reductase holoenzyme in complex with the potent aldose reductase inhibitor fidarestat: implications for inhibitor binding and selectivity, J. Med. Chem. 48 (2005) 5536–5542.

[11] K.V. Ramana, S.K. Srivastava, Aldose reductase: a novel therapeutic target for inflammatory pathologies, Int. J. Biochem. Cell Biol. 42 (2010) 17–20.

[12] R. Ramasamy, I.J. Goldberg, Aldose reductase and cardiovascular diseases, creating human-like diabetic complications in an experimental model, Circ. Res. 106 (2010) 1449–1458.

[13] R. Kikkawa, I. Hatanaka, H. Yasuda, N. Kobayashi, Y. Shigeta, H. Terashima, T. Morimura, M. Tsuboshima, Effect of a new aldose reductase inhibitor,(E)-3-carboxymethyl-5-[(2E)-methyl-3-phenylpropenylidene] rhodanine (ONO-2235) on peripheral nerve disorders in streptozotocin-diabetic rats, Diabetologia 24 (1983) 290–292.

[14] B.L. Mylari, E.R. Larson, T.A. Beyer, W.J. Zembrowski, C.E. Aldinger, M.F. Dee, T.W. Siegel, D.H. Singleton, Novel, potent aldose reductase inhibitors: 3, 4-dihydro-4-oxo-3-[[5-(trifluoromethyl)-2-benzothiazolyl] methyl]-1-phthalazineacetic acid (zopolrestat) and congeners, J. Med. Chem. 34 (1991) 108–122.

[15] T. Asano, Y. Saito, M. Kawakami, N. Yamada, F.C.P.S. Group, Fidarestat (SNK-860), a potent aldose reductase inhibitor, normalizes the elevated sorbitol accumulation in erythrocytes of diabetic patients, J. Diabetes Complicat. 16 (2002) 133–138.

[16] M.C. Van Zandt, M.L. Jones, D.E. Gunn, L.S. Geraci, J.H. Jones, D.R. Sawicki, J. Sredy, J.L. Jacot, A.T. DiCioccio, T. Petrova, Discovery of 3-[(4, 5, 7-trifluorobenzothiazol-2-yl) methyl] indole-N-acetic acid (lidorestat) and congeners as highly potent and selective inhibitors of aldose reductase for treatment of chronic diabetic complications, J. Med. Chem. 48 (2005) 3141–3152.

[17] C. La Motta, S. Sartini, L. Mugnaini, F. Simorini, S. Taliani, S. Salerno, A.M. Marini, F. Da Settimo, A. Lavecchia, E. Novellino, Pyrido [1, 2-a] pyrimidin-4-one derivatives as a novel class of selective aldose reductase inhibitors exhibiting antioxidant activity, J. Med. Chem. 50 (2007) 4917–4927.

[18] O. El-Kabbani, P. Ramsland, C. Darmanin, R.P.T. Chung, A. Podjarny, Structure of human aldose reductase holoenzyme in complex with Statil: an approach to structure-based inhibitor design of the enzyme, Proteins: Struct., Funct., Bioinf. 50 (2003) 230–238.

[19] L. Huang, R. He, W. Luo, Y.-S. Zhu, J. Li, T. Tan, X. Zhang, Z. Hu, D. Luo, Aldo-keto reductase family 1 member B10 inhibitors: potential drugs for cancer treatment, Recent Pat. Anticancer Drug Discov. 11 (2016) 184–196.

[20] O. Gallego, F.X. Ruiz, A. Ardèvol, M. Domínguez, R. Alvarez, A.R. de Lera, C. Rovira, J. Farrés, I. Fita, X. Parés, Structural basis for the high all-trans-retinaldehyde reductase activity of the tumor marker AKR1B10, Proc. Natl. Acad. Sci. USA 104 (2007) 20764–20769.

[21] E. Kropotova, R. Tychko, O. Zinov'eva, A. Zyryanova, S. Khankin, V. Cherkes, V. Aliev, S. Beresten, N.Y. Oparina, T. Mashkova, Downregulation of AKR1B10 expression in colorectal cancer, Mol. Biol. 44 (2010) 216–222.

[22] A. Saeed, Y. Tehseen, H. Rafique, N. Furtmann, J. Bajorath, U. Flörke, J. Iqbal, Benzothiazolyl substituted iminothiazolidinones and benzamido-oxothiazolidines as potent and partly selective aldose reductase inhibitors, Med. Chem. Comm. 5 (2014) 1371–1380.

[23] A. Ibrar, Y. Tehseen, I. Khan, A. Hameed, A. Saeed, N. Furtmann, J. Bajorath, J. Iqbal, Coumarin-thiazole and-oxadiazole derivatives: synthesis, bioactivity and docking studies for aldose/aldehyde reductase inhibitors, Bioorg. Chem. 68 (2016) 177–186.

[24] H.A. Bhatti, Y. Tehseen, K. Maryam, M. Uroos, B.S. Siddiqui, A. Hameed, J. Iqbal, Identification of new potent inhibitor of aldose reductase from Ocimum basilicum, Bioorg. Chem. 75 (2017) 62–70.

[25] H. Andleeb, Y. Tehseen, F. Jabeen, I. Khan, J. Iqbal, S. Hameed, Exploration of thioxothiazolidinone–sulfonate conjugates as a new class of aldehyde/aldose reductase inhibitors: a synthetic and computational investigation, Bioorg. Chem. 75 (2017) 1–15.

[26] M.T. Shehzad, A. Imran, G.S.S. Njateng, A. Hameed, M. Islam, M. al-Rashida, M. Uroos, A. Asari, Z. Shafiq, J. Iqbal, Benzoxazinone-thiosemicarbazones as anti-diabetic leads via aldose reductase inhibition: synthesis, biological screening and molecular docking study, Bioorg. Chem. (2018).

[27] A. Hameed, K.M. Khan, S.T. Zehra, R. Ahmed, Z. Shafiq, S.M. Bakht, M. Yaqub, M. Hussain, A.d.l.V. de León, N. Furtmann, Synthesis, biological evaluation and molecular docking of N-phenyl thiosemicarbazones as urease inhibitors, Bioorg. Chem. 61 (2015) 51–57.

[28] M. Islam, A. Khan, M.T. Shehzad, A. Hameed, N. Ahmed, S.A. Halim, M. Khiat, M.U. Anwar, J. Hussain, R. Csuk, Z. Shafiq, A. Al-Harrasi, Synthesis and characterization of new thiosemicarbazones, as potent urease inhibitors: In vitro and in silico studies, Bioorg. Chem. (2019).

[29] S. Malik, A. Khan, M.M. Naseer, S.U. Khan, A. Ashraf, M. Ashraf, M. Rafiq, K. Mahmood, M.N. Tahir, Z. Shafiq, T. Qamar-un-Nisa, Xanthenone-based hydrazones as potent α-glucosidase inhibitors: synthesis, solid state self-assembly and in silico studies, Bioorg. Chem. 84 (2019) 372–383.

[30] A. Hameed, M. Yaqub, M. Hussain, A. Hameed, M. Ashraf, H. Asghar, M.M. Naseer, K. Mahmood, M. Muddassar, M.N. Tahir, Z. Shafiq, Coumarin-based thiosemicarbazones as potent urease inhibitors: synthesis, solid state self-assembly and molecular docking, RSC Adv. 6 (2016) 63886–63894.

[31] V. Carbone, M. Giglio, R. Chung, T. Huyton, J. Adams, R. Maccari, R. Ottana, A. Hara, O. El-Kabbani, Structure of aldehyde reductase in ternary complex with a 5-arylidene-2, 4-thiazolidinedione aldose reductase inhibitor, Eur. J. Med. Chem. 45 (2010) 1140–1145.